Performance Evaluation of a Moving Horizon Estimator for Multi-Rate Sensor Fusion with Time-Delayed Measurements

Rodolphe Dubois, Sylvain Bertrand, Alexandre Eudes
ONERA - DTIS
F-91123 Palaiseau - France
Email: *firstname.lastname@onera.fr*

***Abstract*—In this paper, the use of a Moving Horizon Estimator (MHE) is investigated to address a class of state estimation problems dealing with multi-rate sensor fusion in presence of time-delayed measurements. As it makes use of a batch of past measurement and state estimates, MHE is indeed a good candidate to deal with "missing" measurements. Nevertheless, since Moving Horizon Estimation relies on solving online an optimization problem to compute the sate estimate, its computational load may be prohibitive for practical implementation to fast dynamical systems. Therefore this paper proposes a computationaly efficient implementation scheme for a variable structure linear MHE dealing with multi-rate time-delayed measurements, in the case where an analytical solution of the underlying optimization problem can be found. A simulation example is considered for performance comparison, in terms of accuracy and computation time, of the proposed MHE with respect to several state-of-the-art estimators.**

I. Introduction

A. Considered problem

Multi-sensor fusion is a widely used approach for state estimation problems. The localization problem of a robot or a drone can for example be addressed by fusing measurements provided by embedded sensors and/or information reconstructed from these measurements. In some cases, the computation time associated to this reconstruction can not be neglected and will result in some time delay between the availability instant of the reconstructed information and the acquisition time associated to the corresponding measurement. This is more specifically the case for multi-rate sensor fusion problems where "time consuming" algorithms (e.g. computer vision) are used online to provide some information to be fused with high rate sensor measurements (e.g. IMU). In addition, acquisition delays may occur when the physical phenomenon to be measured is not instantaneously observable. Delays due to communications may also appear, especially in the case of sensor networks or multi-robot systems where information are transmitted between nodes or vehicles. In all these cases, the performance of the estimation algorithms will suffer from the presence of time delays and degradations in terms of stability of the estimation error or accuracy of the estimate can be observed.

B. Related work

The problem of state estimation with time delayed measurements is often referred to as a "*negative time measurement update problem*" (see [1]) since state estimation of the current state involves past measurements. Different classes of problems can be considered depending on whether delayed measurements come in-sequence or out-of-sequence (see [2]) and whether the measurement delays are known or not. It is the case if measurements are time-stamped, as considered in this paper. Otherwise, the estimation should rely on some probabilistic characterizations of the delays (see [3], [4], [5], [6]). To deal with delayed measurements, some methods are based on the use of predictors to compensate for the delay (see [7], [8], [9]). Another approaches rely on computing an update in the correction term to be applied to the current state estimate (see [10], [2]). A third class of approaches makes use of the delayed measurement in its past context to re-estimate the whole sequence of posterior state estimates (see [6], [11], [12], [13]).

To cope with the (un) availability of several measurements, a buffer can be used to store a finite number of past information (measurements, state estimates). This is in particular the case of Moving Horizon Estimators (MHE) which rely on the resolution of an optimization problem that makes use of measurements over a finite past horizon of time. Although there exist a lot of works in the literature that consider fast MHE algorithms, by ad-hoc optimization procedures (see [14], [15], [16]) or by an adequate formulation of the optimization problem to be solved (see [17]), there exist very few work focusing simultaneously on computational load reduction and multi-rate sensor fusion in presence of time-delayed measurements with this type of estimators. In [18] a variable structure MHE is proposed to cope with time-delayed measurements. Nevertheless implementation to fast dynamical systems and multi-rate measurements are not considered. In [19] a regularization scheme is designed along with a specific cost function in the MHE formulation to adapt the weight associated to missing data, enabling to handle time delays. Computational time is experimentally investigated but in the case of single rate measurements. In [12], an MHE is implemented to fuse IMU and GPS measurements for state estimation of a fixed-wing aircraft. Multiple rates are handled by resampling GPS measurements to the IMU rate. In [20], additional measurements from a pitot-static tube are included in the fusion problem to also estimate wind velocity

and aerodynamic coefficients. Nevertheless, in these last two works, on-line implementation is not really addressed nor possible time-delays in measurements.

C. Contributions

In this paper, we investigate the use of a Moving Horizon Estimator for multi-rate sensor fusion with time-delays. Based on the approach initially proposed in [18] to deal with time delays, a variable structure MHE is used here to both handle multi-rates and time delays. The linear case is addressed in this work to obtain an analytical formulation that is computationally tractable and can easily be applied in real time to fast dynamical systems. To further improve the computation time, a procedure is proposed to perform off-line pre-computations as much as possible and only update online some specific terms that are related to the (un)availability of the measurements over the finite horizon of the MHE.

The rest of the paper is organized as follows. In Section II the problem of interest is defined to which an analytical solution is then derived in Section III. Section IV proposes a procedure to improve computation time. Performance of the proposed MHE is then evaluated in Section V by considering a simple benchmark example and by analyzing accuracy of the estimates and computation time wrt to some state-of-the-art estimators. Concluding remarks are finally proposed in the last section of the paper.

II. Problem statement

A. Moving Horizon Estimators

Consider a general discrete-time dynamic system

$$\mathbf{x_k} = f(\mathbf{x_{k-1}}, \mathbf{u_{k-1}}) + \mathbf{w_{k-1}} \tag{1}$$

and measurement equation

$$\mathbf{z_k} = h(\mathbf{x_k}) + \boldsymbol{\nu_k} \tag{2}$$

where $\mathbf{x_k} \in \mathbb{R}^n$ is the state of the system, $\mathbf{u_k} \in \mathbb{R}^m$ its input, $\mathbf{z_k} \in \mathbb{R}^p$ the vector of measurements at time index k. The process noise $\mathbf{w_k} \in \mathbb{R}^n$ and the measurement noise $\boldsymbol{\nu_k} \in \mathbb{R}^p$ are assumed to be zero mean white Gaussian noises of covariance matrices $\mathbf{Q_k}$ and $\mathbf{R_k}$. Let N be the length of a finite horizon over which the sequences of the system inputs $\mathbf{u_{k-N}^{k-1}} = \{\mathbf{u_{k-N}}, ..., \mathbf{u_{k-1}}\}$ and the available measurements $\mathbf{z_{k-N}^{k}} = \{\mathbf{z_{k-N}}, \dots, \mathbf{z_k}\}$ are assumed to be known. Moving Horizon Estimation consists in computing at time index k the state estimate $\hat{\mathbf{x}}_\mathbf{k} \in \mathbb{R}^n$ by solving the optimization problem

$$\begin{Bmatrix} \hat{\mathbf{x}}_{\mathbf{k-N}} \\ \hat{\mathbf{w}}_{\mathbf{k-N}}^{\mathbf{k-1}} \end{Bmatrix} = \underset{\substack{\mathbf{x_{k-N}} \\ \mathbf{w_{k-N}^{k-1}}}}{\arg\min} \left\| \mathbf{x_{k-N}} - \bar{\mathbf{x}}_{\mathbf{k-N|k}} \right\|^2_{\mathbf{P}^{-1}_{\mathbf{k-N|k}}} + \sum_{i=0}^{N-1} \left\| \mathbf{w_{k-N+i}} \right\|^2_{\mathbf{Q}^{-1}_{\mathbf{k-N+i}}} + \sum_{i=0}^{N} \left\| \mathbf{z_{k-N+i}} - \hat{\mathbf{z}}_{\mathbf{k-N+i}} \right\|^2_{\mathbf{R}^{-1}_{\mathbf{k-N+i}}} \tag{3}$$

where $\mathbf{w_{k-N}^{k-1}} = \{\mathbf{w_{k-N}}, ..., \mathbf{w_{k-1}}\}$ is the sequence of process noises, $\mathbf{x_{k-N}}$ is the horizon front state, $\hat{\mathbf{z}}_{\mathbf{k-N+i}} = h \circ f^{\mathbf{w_{k-N-1+i}}}_{\mathbf{u_{k-N-1+i}}} \circ \cdots \circ f^{\mathbf{w_{k-N}}}_{\mathbf{u_{k-N}}}(\mathbf{x_{k-N}})$ with $f^{\mathbf{w}}_{\mathbf{u}}(\mathbf{x}) = f(\mathbf{x}, \mathbf{u}) + \mathbf{w}$, and $\mathbf{P_{k-N|k}}$ the recursively estimated covariance matrix of $\mathbf{x_{k-N|k}}$. After the optimization is carried out, the prior on $\mathbf{x_{k-N}}$ on $\bar{\mathbf{x}}_{\mathbf{k-N}}$ is propagated through the dynamical model :

$$\bar{\mathbf{x}}_{\mathbf{k+1-N|k-N}} = f(\hat{\mathbf{x}}_{\mathbf{k-N}}, \mathbf{u_{k-N}}) + \hat{\mathbf{w}}_{\mathbf{k-N}} \tag{4}$$

The covariance can be propagated e.g. by using the Extended Kalman Filter's (EKF) covariance prediction and update formulas. The current state estimate is computed as :

$$\hat{\mathbf{x}}_\mathbf{k} = f^{\hat{\mathbf{w}}_{\mathbf{k-1}}}_{\mathbf{u_{k-1}}} \circ \cdots \circ f^{\hat{\mathbf{w}}_{\mathbf{k-N}}}_{\mathbf{u_{k-N}}}(\hat{\mathbf{x}}_{\mathbf{k-N}}) \tag{5}$$

B. Particular forms of the MHE problem

1) MHE with variable structure: As specified in the introduction and introduced in [18], an efficient MHE needs its structure to be variable in order to correctly handle two facts. On one hand, the observation system may be multi-rate, so the MHE needs to integrate measurements acquired at different frequencies. On the other hand, some measurements may be delayed, and so they should be replaced in their context when received.

2) MHE estimation with and without process noise: An approximate form of the MHE can be derived by estimating only $\mathbf{x_{k-N}}$ and omitting the sequence of process noises $\mathbf{w_{k-N}^{k-1}}$. This solution compensates a loss of accuracy for lighter computational load, since the sequence of process noises is the heaviest part of the estimated vector.

III. Analytical solutions in the linear case

A. Discrete LTI system

In the rest of this paper, a linear system as follows will be considered :

$$\mathbf{x_k} = \mathbf{A}\mathbf{x_{k-1}} + \mathbf{B}\mathbf{u_{k-1}} + \mathbf{M}\mathbf{w_k} \tag{6a}$$

$$\mathbf{z_k} = \mathbf{C}\mathbf{x_k} + \boldsymbol{\nu_k} \tag{6b}$$

where $\mathbf{w_k}$ and $\boldsymbol{\nu_k}$ are white Gaussian noises whose covariance matrices are respectively $\mathbf{Q_k}$ and $\mathbf{R_k}$. $\mathbf{u_k}$ is the control input at time step k. $\mathbf{z_k}$ is the measurement vector associated with state $\mathbf{x_k}$, but it may be received at time step $l \geq k$.

B. Derivation of the closed-form solution

In the linear form, the measurement prediction function as well as the dynamical constraints are linear. The optimization problem's cost function, explicitely expressed as a function of $\mathbf{x_{k-N}}$ and $\mathbf{w_{k-N}^{k-1}}$, is convex and thus has a unique solution which can be computed analytically by zeroing its gradient.

1) Closed-form for measurement predictions: Let $\hat{\mathbf{z}}_{\mathbf{k-N}}^{\mathbf{k}}$, $\mathbf{u_{k-N}^{k-1}}$ and $\mathbf{w_{k-N}^{k-1}}$ be the stacked vectors of the sequence of predicted measurements, control inputs and process noises over the horizon. One easily shows that

$$\hat{\mathbf{z}}_{\mathbf{k-N}}^{\mathbf{k}} = \mathbf{M_X}.\mathbf{x_{k-N}} + \mathbf{M_W}.\mathbf{w_{k-N}^{k-1}} + \mathbf{M_U}.\mathbf{u_{k-N}^{k-1}} \tag{7}$$

where the following matrices are defined as follows :

$$\mathbf{M_X} = \begin{bmatrix} (\mathbf{C}\mathbf{A}^N)^T & \cdots & (\mathbf{C}\mathbf{A}^1)^T & (\mathbf{C}\mathbf{A}^0)^T \end{bmatrix}^T \tag{8a}$$

$$\mathbf{M_W} = \begin{bmatrix} \mathbf{CA^0M} & \mathbf{CA^1M} & \cdots & \mathbf{CA^{N-1}M} \\ \vdots & \mathbf{CA^0M} & \cdots & \mathbf{CA^{N-2}M} \\ \vdots & & \ddots & \vdots \\ \vdots & & & \mathbf{CA^1M} \\ \vdots & & & \mathbf{CA^0M} \\ \mathbf{0} & \cdots & \cdots & \mathbf{0} \end{bmatrix} \tag{8b}$$

$$\mathbf{M_U} = \begin{bmatrix} \mathbf{CA^0B} & \mathbf{CA^1B} & \cdots & \mathbf{CA^{N-1}B} \\ \vdots & \mathbf{CA^0B} & \cdots & \mathbf{CA^{N-2}B} \\ \vdots & & \ddots & \vdots \\ \vdots & & & \mathbf{CA^1B} \\ \vdots & & & \mathbf{CA^0B} \\ \mathbf{0} & \cdots & \cdots & \mathbf{0} \end{bmatrix} \tag{8c}$$

with $\mathbf{0}$ being zero matrices of appropriate dimensions.

2) Closed-form for the cost function: By injecting (7) into the cost function expression, and by considering the matrices

$$\mathcal{R}_\mathbf{k} = \text{diag}\left(\mathbf{R_k}, \cdots, \mathbf{R_{k-N}}\right) \tag{9a}$$

$$\mathcal{Q}_\mathbf{k} = \text{diag}\left(\mathbf{Q_{k-1}}, \cdots, \mathbf{Q_{k-N}}\right) \tag{9b}$$

the cost function J_k can be rewritten

$$J_k = \left\|\mathbf{z^k_{k-N}} - \hat{\mathbf{z}}^\mathbf{k}_\mathbf{k-N}\right\|^2_{\mathcal{R}_\mathbf{k}^{-1}} + \left\|\mathbf{w^{k-1}_{k-N}}\right\|^2_{\mathcal{Q}_\mathbf{k}^{-1}} + \left\|\mathbf{x_{k-N|k}} - \bar{\mathbf{x}}_\mathbf{k-N|k}\right\|^2_{\mathbf{P}^{-1}_\mathbf{k-N}} \tag{10}$$

which yields

$$J_k = \begin{bmatrix} \mathbf{x_{k-N}} \\ \mathbf{w^{k-1}_{k-N}} \end{bmatrix}^T \begin{bmatrix} \mathbf{Q_{XX}} & \mathbf{Q_{XW}} \\ \mathbf{Q^T_{XW}} & \mathbf{Q_{WW}} \end{bmatrix} \begin{bmatrix} \mathbf{x_{k-N}} \\ \mathbf{w^{k-1}_{k-N}} \end{bmatrix} + 2\left(\begin{bmatrix} \mathbf{L_{XU}} \\ \mathbf{L_{WU}} \end{bmatrix} \mathbf{u^{k-1}_{k-N}} - \begin{bmatrix} \mathbf{L_{XZ}} \\ \mathbf{L_{WZ}} \end{bmatrix} \mathbf{z^{k-1}_k} - \begin{bmatrix} \mathbf{L_{XX}} \\ \mathbf{L_{WX}} \end{bmatrix} \bar{\mathbf{x}}_\mathbf{k-N|k} \right)^T \begin{bmatrix} \mathbf{x_{k-N}} \\ \mathbf{w^{k-1}_{k-N}} \end{bmatrix} \tag{11}$$

with the following matrices being defined as follows :

$$\begin{aligned} &\mathbf{Q_{XX}} = \mathbf{M^T_X}\mathcal{R}_\mathbf{k}\mathbf{M_X} + \mathbf{P_{k-N}} && \mathbf{Q_{XW}} = \mathbf{M^T_X}\mathcal{R}_\mathbf{k}\mathbf{M_W} \\ &\mathbf{Q_{WW}} = \mathbf{M^T_W}\mathcal{R}_\mathbf{k}\mathbf{M_W} + \mathcal{Q}_\mathbf{k} && \mathbf{L_{XU}} = \mathbf{M^T_X}\mathcal{R}_\mathbf{k}\mathbf{M_U} \\ &\mathbf{L_{WU}} = \mathbf{M^T_W}\mathcal{R}_\mathbf{k}\mathbf{M_U} && \mathbf{L_{XZ}} = \mathbf{M^T_X}\mathcal{R}_\mathbf{k} \\ &\mathbf{L_{WZ}} = \mathbf{M^T_W}\mathcal{R}_\mathbf{k} && \mathbf{L_{XX}} = \mathbf{P_{k-N}} \\ &\mathbf{L_{WX}} = \mathbf{0} \end{aligned} \tag{12}$$

3) Zeroing the gradient: The sufficient and necessary conditions for optimality yield :

$$\begin{bmatrix} \mathbf{Q_{XX}} & \mathbf{Q_{XW}} \\ \mathbf{Q^T_{XW}} & \mathbf{Q_{WW}} \end{bmatrix} \begin{bmatrix} \mathbf{x_{k-N}} \\ \mathbf{w^{k-1}_{k-N}} \end{bmatrix} = \begin{bmatrix} \mathbf{L_{XZ}} \\ \mathbf{L_{WZ}} \end{bmatrix} \mathbf{z^k_{k-N}} - \begin{bmatrix} \mathbf{L_{XU}} \\ \mathbf{L_{WU}} \end{bmatrix} \mathbf{u^{k-1}_{k-N}} + \begin{bmatrix} \mathbf{L_{XX}} \\ \mathbf{0} \end{bmatrix} \bar{\mathbf{x}}_\mathbf{k-N|k} \tag{13}$$

The current estimate is then computed using

$$\hat{\mathbf{x}}_\mathbf{k|k} = \mathbf{A^N}\hat{\mathbf{x}}_\mathbf{k-N|k} + \begin{bmatrix} \mathbf{B} & \mathbf{AB} & \cdots & \mathbf{A^{N-1}B} \end{bmatrix} \mathbf{u^{k-1}_{k-N}} + \begin{bmatrix} \mathbf{M} & \mathbf{AM} & \cdots & \mathbf{A^{N-1}M} \end{bmatrix} \hat{\mathbf{w}}^\mathbf{k-1}_\mathbf{k-N} \tag{14}$$

which is the linear form of equation (5). Note that solving the MHE problem without process noises merely shrinks to solving the following linear system for $\mathbf{x_{k-N}}$:

$$\mathbf{Q_{XX}}.\mathbf{x_{k-N}} = \mathbf{L_{XZ}}.\mathbf{z^k_{k-N}} - \mathbf{L_{XU}}.\mathbf{u^{k-1}_{k-N}} + \mathbf{L_{XX}}.\bar{\mathbf{x}}_\mathbf{k-N|k} \tag{15}$$

IV. Implementation

The implementation of the MHE should take into account the variability of the problem formulation from one time step to another because of the unavailability of some measurements. Impacting the unavailability of measurement $\mathbf{z_{k-N+i}}$ boils down to ignore every matrix term in equation (13) which relates to it. This is equivalent to ignore every matrix block in which one the weighting matrix $\mathbf{R_{k-N+i}}$ does appear. Indeed, one remarks that every matrix defined in (12) breaks down into a sum of "elementary" matrices which should be selected according to available measurements at time step k. Furthermore, all those elementary matrices can be pre-computed off-line. Therefore, the proposed implementation involves building the matrices of the system (13) at each time step by adding those pre-computed matrix terms according to available measurements.

A. Matrices used in the problem formulation

Each of the matrix block defined in equation (12) is analyzed so as to be split into a sum of matrix terms to highlight its relation to the availability of measurements over the horizon. Matrices issued from such a decomposition should then be handled in appropriate structures to be used at proper moments. The contributions of each measurement to the the block matrices defined in equation (12) appear explicitly in the decomposition of those matrices given below :

$$\mathbf{M_{XX}} = \mathbf{P_{k-N}} + \sum_{i=0}^{N} (\mathbf{CA^{N-i}})^T \mathbf{R_{k-i}} (\mathbf{CA^{N-i}}) \tag{16a}$$

$$\mathbf{M_{XW}} = \sum_{i=0}^{N-1} \left(\mathbf{CA^i}\right)^T \mathbf{R_{k-i}} (\mathbf{M_W})_{(i:)} \tag{16b}$$

$$\mathbf{M_{WW}} = \mathcal{Q}_\mathbf{k} + \sum_{i=0}^{N-1} ((\mathbf{M_W})_{(i:)})^T \mathbf{R_{k-i}} (\mathbf{M_W})_{(i:)} \tag{16c}$$

$$\mathbf{L_{XU}} = \sum_{i=0}^{N} ((\mathbf{M_X})_{(i:)})^T \mathbf{R_{k-i}} (\mathbf{M_U})_{(i:)} \tag{16d}$$

$$\mathbf{L_{WU}} = \sum_{i=0}^{N-1} ((\mathbf{M_W})_{(i:)})^T \mathbf{R_{k-i}} (\mathbf{M_U})_{(i:)} \tag{16e}$$

$$\mathbf{L_{XZ}} = \sum_{i=0}^{N} \left(\mathbf{CA^i}\right)^T \mathbf{R_{k-i}} \tag{16f}$$

$$\mathbf{L_{WZ}} = \sum_{i=0}^{N} ((\mathbf{M_W})_{(i:)})^T \mathbf{R_{k-i}} \tag{16g}$$

where the subscripts $\cdot_{(i:)}$ refer to the i^{th} block line of the subscripted block matrices. All the summands can be pre-computed and arranged into properly indexed grids, so that to be added to the corresponding block matrix to build the system (13) when their associated measurement is available within

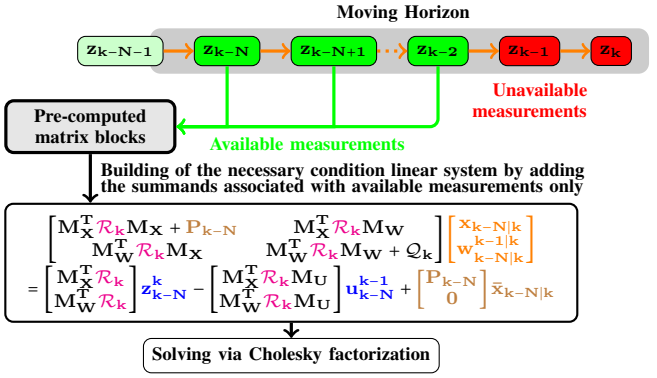

Fig. 1: Implementation scheme of the linear moving horizon estimator from the closed-form solution of the optimization problem

the horizon. Note that for the matrices $\mathbf{M_{XW}}$, $\mathbf{M_{WW}}$ and $\mathbf{L_{WU}}$, no matrix block is associated to the measurement $\mathbf{z_{k-N}}$. At each time-step, matrices $\mathbf{M_{XX}}$ and $\mathbf{M_{WW}}$ are initialized respectively at $\mathbf{P_{k-N}}$ and $\mathcal{Q}_\mathbf{k}$.

B. Proposed procedure for computation time improvement

The proposed procedure is illustrated in Figure 1. It relies on expressing the MHE problem by shaping directly the linear system characterizing its solutions. As previously mentioned, in the block matrices of the linear equation (13), the contributions of each measurement within the horizon is identified and extracted. This allows to build the linear system characterizing the solution of the MHE problem which is exactly adapted to the set of available measurements over the horizon, and then take advantage of the closed-form the solution to efficiently compute the estimates of $\mathbf{x_{k-N}}$ and $\mathbf{w}^{\mathbf{k-1}}_{\mathbf{k-N}}$ via Cholesky decomposition, and then $\hat{\mathbf{x}}_\mathbf{k}$ from (14).

V. Performance evaluation

A. Considered study case

As a study case, a simplified model of the translational dynamcis of a drone is considered:

$$\dot{\mathbf{x}} = \mathbf{v} \tag{17a}$$

$$\dot{\mathbf{v}} = \mathbf{a} \tag{17b}$$

where $\mathbf{x}$ is the position of the drone, $\mathbf{v}$ its velocity, and $\mathbf{a}$ its acceleration. Measurements are obtained by an accelerometer and a visual odometry algorithm, which are simply modeled as follows

$$\mathbf{a_m} = \mathbf{a} + \mathbf{a_b} + \mathbf{a}_\eta \tag{18}$$

$$\mathbf{p_m} = \mathbf{p} + \mathbf{p}_\eta \tag{19}$$

$\mathbf{a_m}$ is the acceleration measured by the accelerometer[1] and $\mathbf{p_m}$ is the position measured by the odometer ; $\mathbf{a_b}$ is the accelerometer bias, and $\mathbf{a}_\eta$ and $\mathbf{p}_\eta$ are white Gaussian noises whose covariance matrices are respectively $\mathbf{R_{acc}}$ and $\mathbf{R_{odo}}$. The estimation model is obtained via Euler integration at sampling period T_e:

$$\mathbf{p_k} = \mathbf{p_{k-1}} + T_e \cdot \mathbf{v_{k-1}} \tag{20a}$$

$$\mathbf{v_k} = \mathbf{v_{k-1}} + T_e \cdot \left(\mathbf{a_{mk-1}} - \mathbf{a_{bk-1}} - \mathbf{a}_{\eta\mathbf{k-1}}\right) \tag{20b}$$

Defining $\mathbf{x_k} = \begin{bmatrix} \mathbf{p_k^T} & \mathbf{v_k^T} & \mathbf{a_b}_\mathbf{k}^\mathbf{T} \end{bmatrix}^\mathbf{T}$, the estimation model can be written as

$$\mathbf{x_k} = \mathbf{A}\mathbf{x_{k-1}} + \mathbf{B}\mathbf{u_{k-1}} + \mathbf{M}\mathbf{w_{k-1}} \tag{21}$$

with the following matrices

$$\mathbf{A} = \begin{bmatrix} \mathbf{I_{3\times3}} & T_e \cdot \mathbf{I_{3\times3}} & \mathbf{0_{3\times3}} \\ \mathbf{0_{3\times3}} & \mathbf{I_{3\times3}} & \mathbf{0_{3\times3}} \\ \mathbf{0_{3\times3}} & \mathbf{0_{3\times3}} & \mathbf{I_{3\times3}} \end{bmatrix} \tag{22a}$$

$$\mathbf{B} = \begin{bmatrix} \mathbf{0_{3\times3}} \\ T_e \cdot \mathbf{I_{3\times3}} \\ \mathbf{0_{3\times3}} \end{bmatrix} \qquad \mathbf{M} = \begin{bmatrix} \mathbf{0_{3\times3}} \\ \mathbf{I_{3\times3}} \\ \mathbf{0_{3\times3}} \end{bmatrix} \tag{22b}$$

and considering the accelerometer measurement as input, $\mathbf{u_k} = \mathbf{a_m}$, which is assumed to be available at each time step. The process noise $\mathbf{w_k}$ has a covariance matrix $T_e^2\mathbf{R_{acc}}$. The measurement equation is:

$$\mathbf{z_k} = \mathbf{C}\mathbf{x_k} + \boldsymbol{\nu_k} \tag{23}$$

with $\mathbf{C} = \begin{bmatrix} \mathbf{I_{3\times3}} & \mathbf{0_{3\times3}} & \mathbf{0_{3\times3}} \end{bmatrix}$, and $\boldsymbol{\nu_k}$ the measurement noise of covariance matrix $\mathbf{R_{odo}}$. Numerical values of process and measurement noise covariances, sensor rates and sampling period can be found in Table I.

The position measurement from visual odometry is supposed to be affected by delays, because of the time needed to process the acquired image, which commonly involves extracting feature points from the images and matching them with features extracted from previous images in order to estimate the relative homogeneous transformations between the successive frames.[2]

B. Comparison filters

The proposed approach is evaluated against other filters which are similar to the MHE in the sense they also replace the delayed measurements in their context and re-estimate the sequence up to the current estimate. Performance evaluation of the proposed MHE, without process noises (denoted **MHE**) and with process noise (denoted **MHEN**), are carried against a classical Kalman Filter (**KF**), a Circular Iterated Extended Kalman Filter (**CIEKF**) proposed in [11], an Augmented State Kalman Filter (**ASKF**) described in [13] and [6] and a Receding Horizon Kalman Filter (**RHKF**) described in [21]. The main characteristics of the last three filters are summed up as

[1]Note that measurement from a strapped-down accelerometer is usually provided in a body-frame and position measurement from visual odometry in a global referene frame. For simplicity reasons, it is assumed here that acceleration measurements are directly provided in the global reference frame.

[2]Here, for the sake of simplicity, multi rates are only considered between the input and the measurement vectors of the system. Multi rates between two contributions to the components of the measurement vector could have also been considered, e.g. adding a GPS position measurement with its own rate, with few changes to the approach.

- CIEKF : given a delayed measurement, it re-estimates the whole sequence of states in between the state corresponding to the measurement and the current one.
- RHKF : it shows the same architecture as a classical KF but augments its state vector to include states over a finite past time horizon. Its augmented state dynamics involves predicting the whole sequence of states at each timestep.
- ASKF : it is quite similar to the RHKF, except that its augmented dynamics only involves translating all the states but the front state which is predicted.

C. Estimation accuracy and computation time

The metric used to evaluate the accuracy of a given filter $\mathcal{F} \in \{\text{KF}, \text{MHE}, \text{MHEN}, \text{CIEKF}, \text{RHKF}, \text{ASKF}\}$ is the *Root Mean Squared Error* (RMSE) of the estimate, defined as

$$\text{RMSE}_{\mathcal{F}}(T) = \sqrt{\sum_{i=0}^{T} \left\| \hat{\mathbf{x}}_\mathbf{i} - \mathbf{x}_\mathbf{i} \right\|^2} \tag{24}$$

where $\{\mathbf{x_i}\}_{i=0,\dots,T}$ and $\{\hat{\mathbf{x}}_\mathbf{i}\}_{i=0,\dots,T}$ respectively stand for the sequence of states and estimates over the time window $[0, T]$. In order to compare the performance of the filters against a same reference, chosen as the Kalman Filter with the same delay assumption on measurements, the ratio

$$\rho_{\mathcal{F}}(T) = \log_{10}\left(\frac{\text{RMSE}_{\mathcal{F}}(T)}{\text{RMS}_{\text{KF}}(T)}\right) \tag{25}$$

is defined for any given filter $\mathcal{F}$. If the ratio $\rho_{\mathcal{F}}$ is negative, then the filter $\mathcal{F}$ is more accurate than the classical KF. If $\rho_{\mathcal{F}_i} < \rho_{\mathcal{F}_j}$, then the filter $\mathcal{F}_i$ is more accurate than the filter $\mathcal{F}_j$. Another performance index considered for each filter is the computation time which is analyzed by computing the $\log_{10}$ of the mean number of iterations per second of the filter over the whole duration of the simulated trajectory.

D. Simulation results

First, a reference trajectory consisting in an ascending helix is simulated over T = 100s for the drone along with the corresponding sensor measurements using parameter values given in Table I. Several simulations have been performed for different values of the delay δ affecting the position measurement provided by visual odometry, from 0s (no delay) up to 1s, by 50ms increments. For each value of the measurement delay δ, all the filters are also tested for different values of the horizon length N. Figure 2 presents a selection of the obtained simulated results. The ratio $\rho_{\mathcal{F}}$ is plotted for each filter $\mathcal{F}$ with respect to δ, and for different values of N. Only the position component of the state is considered in the RMSE computations for simplicity of analysis, but similar results are obtained when also considering the velocity and accelerometer bias components of the state.

Figures 2a, 2b, 2c, 2d and 2e show the evolution of $\rho_{\mathcal{F}}$ respectively for the CIEKF, ASKF, RHKF, MHE and MHEN filters. MHE and MHEN have been tested with the proposed implementation. The CIEKF, ASKF and RHKF all demonstrate a better accuracy than the Kalman Filter regarding position RMSE, with an average $\rho_{\mathcal{F}}$ ratio close to -1.5. For these three filters, the results are quite similar whatever the value of N. Both MHE and MHEN also show better accuracy than the Kalman Filter, despite a sudden decrease of performance when the measurement delay δ becomes comparable to the time horizon $N.T_e$. MHEN proves to be the most accurate of all the tested filters, with values for the $\rho_{\mathcal{F}}$ ratio down to -2.9.

Quantity	**Notation and Value**
Integration step	T_e = 0.01 s
IMU frequency	f_{IMU} = 100 Hz
Visual odometer frequency	f_{ODO} = 10 Hz
Accelerometer covariance	$\mathbf{R_{acc}} = (1e^{-3})^2\mathbf{I_{3\times3}}$ m^{2}s^{-4}
Accelerometer bias	$\mathbf{a_b} = 1e^{-2}\mathbf{1}$ m.s^{-2}
Visual odometer covariance	$\mathbf{R_{odo}} = (1e^{-3})^2\mathbf{I_{3\times3}}$ m^2
Simulation time horizon	T = 100 s

TABLE I: Main simulation parameters

Some elements of interest for computation time analysis are presented in Table II. For each tested filter, the minimum and maximum values, respectively denoted by I^{min} and I^{max}, of the $\log_{10}$ of the mean number of iterations per second is presented. They are computed over the set of all tested values for (N, δ). In order to assess real time feasibility, in the sense that computation time is lower than the sampling period T_e, two other performance indexes are introduced. The maximum possible value of N for which real time is possible $\forall\delta$ values tested is denoted N_{RT}^{max}. The maximum possible value of δ that can be handled such that there exists a value for N ensuring real time capability is denoted δ_{RT}^{max}. The corresponding value of N is denoted $N_{\delta_{RT}^{max}}$. These results illustrate that the proposed MHE implementation is compatible with real time requirements.

Filter $\mathcal{F}$	$\mathbf{I^{min}}$	$\mathbf{I^{max}}$	$\mathbf{N_{RT}^{max}}$	$\delta_{\mathbf{RT}}^{\mathbf{max}}$	$\mathbf{N}_{\delta_{\mathbf{RT}}^{\mathbf{max}}}$
CIEKF	3.9	4.6	$\forall N$	$\forall\delta$	×
ASKF	0.6	2.2	20	0.15s	20
RHKF	1	3	30	0.35s	40
MHE	2.47	2.58	$\forall N$	$\forall\delta$	×
MHEN	1.8	2.3	70	0.75s	80

TABLE II: Computation time analysis

VI. Conclusion

The contributions of this work are twofold. First, based on the work of [18], a variable structure MHE has been proposed for state estimation of LTI systems when dealing both with time-delayed measurements and multi-rate sensors. Second, a computationally efficient implementation scheme has been proposed enabling to perform offline pre-computations as much as possible. Performance analysis has been carried out in terms of estimate accuracy and computation time by comparing the considered MHE strategy to some other filters of the literature also meant to handle time delays. For that purpose, a simple simulation example has been considered. The results showed that it is possible to achieve better estimation accuracy with the MHE and that the proposed implementation allows real-time implementation to fast dynamical systems.

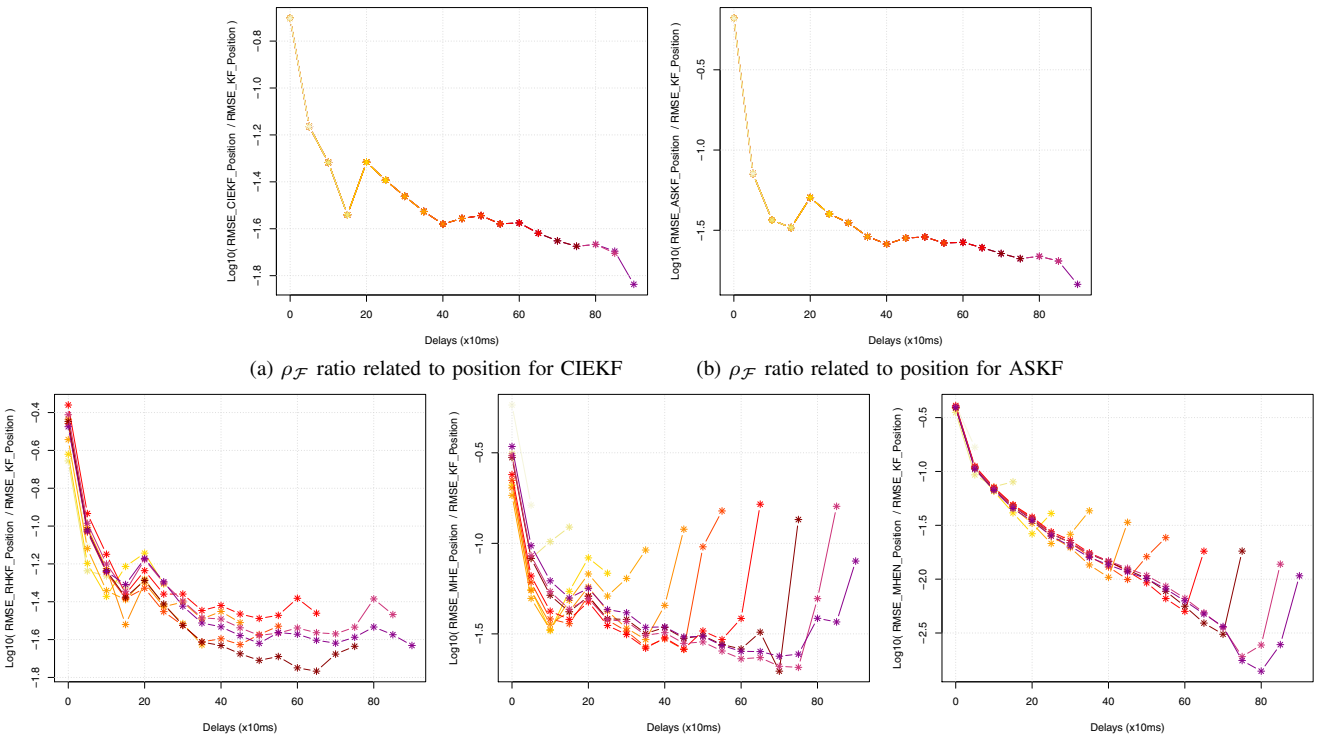

(a) $\rho_{\mathcal{F}}$ ratio related to position for CIEKF (b) $\rho_{\mathcal{F}}$ ratio related to position for ASKF

(c) $\rho_{\mathcal{F}}$ ratio related to position for RHKF (d) $\rho_{\mathcal{F}}$ ratio related to position for MHE (e) $\rho_{\mathcal{F}}$ ratio related to position for MHEN

Time horizons: 100 ms 200 ms 300 ms 400 ms 500 ms 600 ms 700 ms 800 ms 900 ms 1000 ms

Fig. 2: Simulation results for accuracy analysis of the different filters

REFERENCES

[1] Y. Bar-Shalom, "Update with out-of-sequence measurements in tracking: exact solution," *IEEE Transactions on aerospace and electronic systems*, vol. 38, no. 3, pp. 769–777, 2002.

[2] S. Zhang and Y. Bar-Shalom, "Optimal update with multiple out-of-sequence measurements with arbitrary arriving order," *IEEE Transactions on Aerospace and Electronic Systems*, vol. 48, no. 4, pp. 3116–3132, October 2012.

[3] A. K. Yadav, V. K. Mishra, A. K. Singh, and S. Bhaumik, "Unscented Kalman filter for arbitrary step randomly delayed measurements," in *2017 Indian Control Conference (ICC)*, Jan 2017, pp. 82–86.

[4] S. J. Julier and J. K. Uhlmann, "Fusion of time delayed measurements with uncertain time delays," in *Proceedings of the 2005 American Control Conference.*, June 2005, pp. 4028–4033 vol. 6.

[5] Y. Yang, M. Fu, and H. Zhang, "State estimation subject to random network delays without time stamping," in *9th Asian Control Conference (ASCC)*, June 2013, pp. 1–6.

[6] M. Choi, J. Choi, and W. K. Chung, "State estimation with delayed measurements incorporating time-delay uncertainty," *IET Control Theory Applications*, vol. 6, no. 15, pp. 2351–2361, Oct 2012.

[7] A. Khosravian, J. Trumpf, R. Mahony, and T. Hamel, "Recursive attitude estimation in the presence of multi-rate and multi-delay vector measurements," in *2015 American Control Conference (ACC)*, July 2015, pp. 3199–3205.

[8] T. Ahmed-Ali, E. Cherrier, and F. Lamnabhi-Lagarrigue, "Cascade high gain predictors for a class of nonlinear systems," *IEEE Transactions on Automatic Control*, vol. 57, no. 1, pp. 221–226, Jan 2012.

[9] A. Germani, C. Manes, and P. Pepe, "A new approach to state observation of nonlinear systems with delayed output," *IEEE Transactions on Automatic Control*, vol. 47, no. 1, pp. 96–101, Jan 2002.

[10] T. D. Larsen, N. A. Andersen, O. Ravn, and N. K. Poulsen, "Incorporation of time delayed measurements in a discrete-time Kalman filter," in *Proceedings of the 37th IEEE Conference on Decision and Control*, vol. 4, Dec 1998, pp. 3972–3977 vol.4.

[11] S. Lynen, M. W. Achtelik, S. Weiss, M. Chli, and R. Siegwart, "A robust and modular multi-sensor fusion approach applied to mav navigation," in *2013 IEEE/RSJ International Conference on Intelligent Robots and Systems*, Nov 2013, pp. 3923–3929.

[12] T. Polóni, B. Rohal-Ilkiv, and T. A. Johansen, "Moving horizon estimation for integrated navigation filtering," *IFAC-PapersOnLine*, vol. 48, no. 23, pp. 519 – 526, 2015.

[13] S. Challa, R. J. Evans, and X. Wang, "A bayesian solution and its approximations to out-of-sequence measurement problems," *Information Fusion*, vol. 4, no. 3, pp. 185 – 199, 2003.

[14] M. Diehl, H. J. Ferreau, and N. Haverbeke, *Efficient Numerical Methods for Nonlinear MPC and Moving Horizon Estimation*. Berlin, Heidelberg: Springer Berlin Heidelberg, 2009, pp. 391–417.

[15] B. Houska, H. Ferreau, and M. Diehl, "ACADO Toolkit – An Open Source Framework for Automatic Control and Dynamic Optimization," *Optimal Control Applications and Methods*, vol. 32, no. 3, pp. 298–312, 2011.

[16] H. J. Ferreau, T. Kraus, M. Vukov, W. Saeys, and M. Diehl, "High-speed moving horizon estimation based on automatic code generation," in *IEEE 51st IEEE Conference on Decision and Control (CDC)*, Dec 2012, pp. 687–692.

[17] R. Suwantong, S. Bertrand, D. Dumur, and D. Beauvois, "Stability of a nonlinear moving horizon estimator with a pre-estimating observer," in *2014 IEEE American Control Conference*, 2014.

[18] F. Valencia, J. D. López, A. Márquez, and J. J. Espinosa, "Moving horizon estimator for measurement delay compensation in model predictive control schemes," in *50th IEEE Conference on Decision and Control and European Control Conference*, Dec 2011, pp. 6678–6683.

[19] T. A. Johansen, D. Sui, and N. R., "Regularized nonlinear moving-horizon observer with robustness to delayed and lost data," *IEEE Transactions on Control Systems Technology*, vol. 21, no. 6, pp. 2114–2128, 2013.

[20] A. Wenz and T. A. Johansen, "Estimation of wind velocities and aerodynamic coefficients for uavs using standard autopilot sensors and moving horizon estimator," in *Internation Conference on Unmanned Aircradt Systems*, 2017, pp. 1267–1276.

[21] R. Rengaswamy, S. Narasimhan, and V. Kuppuraj, "Receding-horizon Nonlinear Kalman (RNK) filter for state estimation," *IEEE Transactions on Automatic Control*, vol. 58, no. 8, pp. 2054–2059, Aug 2013.